

Robust Finite-Time Zeroing Neural Networks With Fixed and Varying Parameters for Solving Dynamic Generalized Lyapunov Equation

Qiuyue Zuo, Kenli Li[✉], *Senior Member, IEEE*, Lin Xiao[✉], and Keqin Li[✉], *Fellow, IEEE*

Abstract—For solving dynamic generalized Lyapunov equation, two robust finite-time zeroing neural network (RFTZNN) models with stationary and nonstationary parameters are generated through the usage of an improved sign-bi-power (SBP) activation function (AF). Taking differential errors and model implementation errors into account, two corresponding perturbed RFTZNN models are derived to facilitate the analyses of robustness on the two RFTZNN models. Theoretical analysis gives the quantitatively estimated upper bounds for the convergence time (UBs-CT) of the two derived models, implying a superiority of the convergence that varying parameter RFTZNN (VP-RFTZNN) possesses over the fixed parameter RFTZNN (FP-RFTZNN). When the coefficient matrices and perturbation matrices are uniformly bounded, residual error of FP-RFTZNN is bounded, whereas that of VP-RFTZNN monotonically decreases at a super-exponential rate after a finite time, and eventually converges to 0. When these matrices are bounded but not uniform, residual error of FP-RFTZNN is no longer bounded, but that of VP-RFTZNN still converges. These superiorities of VP-RFTZNN are illustrated by abundant comparative experiments, and its application value is further proved by an application to robot.

Index Terms—Dynamic generalized Lyapunov equation, finite-time convergence, robustness, varying parameter, zeroing neural network (ZNN).

I. INTRODUCTION

LYAPUNOV equation is applied prevalently in scientific and electronic engineering fields [1], [2] and works a fairly significant role in controller design and system stability [3]–[5]. Large quantities of strategies, which can be

Manuscript received 4 April 2019; revised 16 October 2020 and 30 March 2021; accepted 26 May 2021. Date of publication 18 June 2021; date of current version 1 December 2022. This work was supported in part by the National Natural Science Foundation of China under Grant 61866013, Grant 61625202, and Grant 61860206011; and in part by the Natural Science Foundation of Hunan Province of China under Grant 2021JJ20005, Grant 18A289, Grant 2018TP1018, and Grant 2018RS3065. (Corresponding authors: Kenli Li; Lin Xiao.)

Qiuyue Zuo and Kenli Li are with the College of Computer Science and Electronic Engineering, Hunan University, Changsha 410082, China (e-mail: zuoqiuyue@hnu.edu.cn; kkl@hnu.edu.cn).

Lin Xiao is with the Hunan Provincial Key Laboratory of Intelligent Computing and Language Information Processing, MOE-LCSM, Hunan Normal University, Changsha 410081, China, and also with Hunan Xiangjiang Artificial Intelligence Academy, Changsha, Hunan 410081, China (e-mail: xiaolin860728@163.com).

Keqin Li is with the College of Computer Science and Electronic Engineering, Hunan University, Changsha 410082, China, and also with the Department of Computer Science, State University of New York, New Paltz, NY 12561 USA (e-mail: lik@newpaltz.edu).

Color versions of one or more figures in this article are available at <https://doi.org/10.1109/TNNLS.2021.3086500>.

Digital Object Identifier 10.1109/TNNLS.2021.3086500

classified into iterative algorithms [6]–[8] and neural dynamics [9]–[11], are adopted to settle the solution of Lyapunov equation in real time. Because those matrix equation-solving tasks with high-dimensional coefficients are time consuming for iterative approaches based on the serial-processing manner as reported in [6], researchers make a tremendous development in neural networks. Originating from Hopfield neural networks, which was first introduced by Hopfield in 1982 [12], [13], recurrent neural networks [14], [15], including gradient-based neural networks (GNNs) and ZNNs, arise wide interest in theoretical research and practical application. For their parallel processing and distributed storage nature, they are elegantly applied to solve various kinds of essential mathematical solving issues.

It can be seen from [9] and [11] that GNN performs well when dealing with static Lyapunov equation. However, as for dynamic Lyapunov equation like in [10] and [16], continuous GNNs, which employ an L_2 -norm-based scalar-valued energy function, bring with lagging-behind errors between the state solutions and the theoretical solution to the target problem [10], [11]. Some discontinuous GNNs are conducted by adopting the gradient of a nonsmooth energy function, which is defined on the basis of the nonsmooth L_1 -norm. As in [17], a discontinuous GNN was established by the subdifferential with regard to the state variables of an L_1 -norm-based energy function. The author claimed that, if the penalty parameter surpasses a specific threshold, the adopted network will reach the target solution in finite time. Hence, for better tracing the target solution, the design parameter should be set as large as the estimated threshold required and as the given hardware permitted. However, it can be difficult to be satisfied and may result in over-fitting in some application scenarios.

Look back to the continuous GNNs, the main reason they fail when dealing with dynamic solutions is that they normally exploit the error matrix norm as the optimization index without making the most of the derivative information of time-varying coefficient matrices. For this reason, a ZNN model, which uses an error vector to record the distance between neural state and target solution to facilitate the usage of derivative information of coefficient matrices in the target problem, is developed to address various time-varying equation-solving problems and succeeds in eliminating the lagging error [10], [11].

It is observed that many researchers have devoted a lot to accelerate the convergence rate of ZNN during the past decades. One of the most basic methods is to apply effi-

cient nonlinear AFs to the conventional ZNN (CZNN). It is worth mentioning that all of AFs before Li *et al.* [18], [19] can expedite the convergence velocity gradually but still keep the defect of infinite-time convergence, which is fairly unpractical to tackle real-time equation solving problems with strict requirements in practical applications. Li *et al.* [18] first proposed a sign-bi-power (SBP) activation function (AF) (SBP-AF) to optimize convergence rate of CZNN and succeeded to achieve finite-time convergence. However, a tremendous amount of data will be generated during the procedure of computer simulations if SBP-AF is applied. Simplified SBP-AFs were thus considered to enhance convergence performance of the neural dynamics in [20] and [21]. After that, a ZNN with fixed parameter activated by a simplified SBP-AF (SSBP-AF) in [20] was proposed to solve DLE in real time [16].

In the implementation process, perturbations resulted from various factors are tricky but inevitable. Most of neural dynamics proposed in studies are efficient under ideal conditions, but that changes when perturbations exist. Some of them with poor robustness are sensitive to perturbations, which are usually deemed as omnipresent backgrounds during computer simulations [20], [22]. Over the past years, many researchers have developed various methods such as proportion-integration-differentiation (PID) controller [23]–[25], and varying parameter [26]–[28], to endow neural networks with robustness. Although the integration item often brings an excellent property of noise suppression, the side effect of time delay (a slight concussion emerging before convergence) going with it is prone to blight simulation results in perturbation-free condition [23], [25]. In consideration of the basic idea of varying parameter methods, which perform as automatically magnifying actual parameters over time, dynamic parameters growing over time can eliminate this flaw and bring in noise tolerance [26], [28]. The accompanying faster convergence also makes it more suitable for the actual situation.

Different from [10], [11] and [16], this work aims to solve dynamic generalized Lyapunov equation (DGLE). The standard Lyapunov equation in [10], [11] and [16] is actually a special case of DGLE. But converting a DGLE into standard form involves the inversion of a matrix. Hence, it is more general to solve DGLE directly. In this work, we creatively put forward an approach converting fixed parameter to exponential-type varying parameter to speed up the convergence and resist the inevitable perturbations. Except for the comparison about upper bounds for the convergence time (UBs-CT) for the fixed-parameter robust finite-time zeroing neural network (RFTZNN) (FP-RFTZNN) model and varying-parameter RFTZNN (VP-RFTZNN) model, their robustness is also verified and compared through taking differential and implementation errors into consideration. For all we know, it is the first time to analytically compare the FP-RFTZNN model and such a novel VP-RFTZNN model in the terms of convergence time and robustness for solving DGLE. Therefore, it is worthwhile to make a synopsis of major contributions to this work.

- 1) Two RFTZNN models with fixed and varying parameters are designed for solving DGLE. By taking differential errors and implementation errors into account, the corresponding perturbed RFTZNN models are proposed.
- 2) The finite-time convergence of two RFTZNN models is proven through theoretical analyses. And their UBs-CT, which in theory reveal the great advantage of VP-RFTZNN over FP-RFTZNN, are quantitatively estimated.
- 3) As proved, residual error of perturbed VP-RFTZNN converges to 0 if both coefficient matrices and perturbation matrices are bounded, whereas that of perturbed FP-RFTZNN is bounded only if they are uniformly bounded.
- 4) The residual error of perturbed VP-RFTZNN is qualitatively proved to either monotonically decrease to an interval in a finite time at a super-exponential convergence rate and stay within it all time after that, or decrease to 0 monotonically and super-exponentially.
- 5) In numerical experiment, the so-called PID-type ZNN (PIDT-ZNN), which is known for its good noise tolerance, is used as the reference object to highlight the performance of two RFTZNN models.

The reminder of this article is composed of six parts. DGLE and CZNN models are formulated in Section II. Section III discusses the performance of FP-RFTZNN in terms of convergence and robustness, and Section IV focuses on that of VP-RFTZNN. An example of solving DGLE with two RFTZNN models is given in Section V, and an application to robot is presented there. At last, a brief conclusion emphasizing on the main results and contributions is drawn in section VI.

II. PROBLEM FORMULATION AND PRELIMINARIES

At the beginning, some mathematical notations used in this work are necessary to be defined. \mathbb{R} represents the set of real numbers and \mathbb{Z} stands for the set of integer numbers. E_2 denotes a matrix with all elements equal to 1. For a matrix $A \in \mathbb{R}^{m \times n}$: $\text{vec}(A)$ is a column vector generated by stacking the column of A ; $\|A\|_F$ denotes the Frobenius norm; and A_{ij} denotes the element of A on row i and column j . The Kronecker product $A \otimes B$, where $B \in \mathbb{R}^{p \times q}$, is defined as

$$A \otimes B = \begin{bmatrix} a_{11}B & a_{12}B & \cdots & a_{1n}B \\ a_{21}B & a_{22}B & \cdots & a_{2n}B \\ \vdots & \vdots & \ddots & \vdots \\ a_{m1}B & a_{m2}B & \cdots & a_{mn}B \end{bmatrix}.$$

$\|\cdot\|_1$ denotes the 1-norm of a vector and $\|\cdot\|_2$ denotes the 2-norm of a vector or the induced 2-norm of a matrix.

This work aims to solve the following DGLE:

$$A^T(t)X(t)B(t) + B^T(t)X(t)A(t) = -C(t) \quad (1)$$

where $X(t) \in \mathbb{R}^{n \times n}$ is unknown. Coefficient matrices $A(t)$, $B(t)$, and $C(t)$ are assumed to be smooth and valued in $\mathbb{R}^{n \times n}$. For ensuring the existence and uniqueness of $X(t)$, a sufficient and necessary condition [29] is cited as follows.

Assumption 1: For any $t > 0$, the matrix pencil $\lambda B(t) - A(t)$ is regular, that is, there must be at least one λ such

that $|\lambda B(t) - A(t)| \neq 0$, and all of its eigenvalues are finite. Besides, $\lambda_i + \bar{\lambda}_j \neq 0$ holds for any two eigenvalues λ_i and $\bar{\lambda}_j$ with $i, j \in \{1, 2, \dots, n\}$.

By letting $M(t) = B^T(t) \otimes A^T(t) + A^T(t) \otimes B^T(t)$, (1) is vectorized as $M(t)x(t) = -c(t)$, where $x(t) = \text{vec}(X(t))$ and $c(t) = \text{vec}(C(t))$. According to [29], (1) is uniquely solvable if and only if $M(t)$ is nonsingular for any t . Hence, under *Assumption 1*, $M(t)$ is invertible.

Here, we present the design process of CZNN for solving (1) as follows:

- 1) Define the following error matrix to record the solution:

$$E(t) = A^T(t)X(t)B(t) + B^T(t)X(t)A(t) + C(t). \quad (2)$$

- 2) Design an evolution formula for $E(t)$

$$dE(t)/dt = -\gamma E(t) \quad (3)$$

where $\gamma > 0$ is an adjustable parameter.

- 3) By substituting (2) into (3), the nonlinear CZNN model is derived as

$$\begin{aligned} & A^T \dot{X}B + B^T \dot{X}A \\ &= -\dot{A}^T X B - A^T X \dot{B} - \dot{B}^T X A \\ & \quad - B^T X \dot{A} - \dot{C} - \gamma (A^T X B + B^T X A + C) \end{aligned} \quad (4)$$

where the time variable t is omitted for ease of writing.

The following lemma indicates the dynamic property of model (4) while solving (1).

Lemma 1 [11]: Given dynamic matrices $A(t)$, $B(t)$, and $C(t)$, which are assumed to satisfy *Assumption 1*, its state matrix $X(t)$ of CZNN (4) converges to the theoretical solution of (1) globally and exponentially.

III. FP-RFTZNN MODEL

In this section, FP-RFTZNN and its perturbed model are formulated and studied. The finite-time convergence of FP-RFTZNN is described by a quoted theorem without proof, whereas its robustness is confirmed theoretically by the analysis of its perturbed model.

A. Design of FP-RFTZNN and Its Perturbed Version

By applying the SSBP-AF $F(\cdot)$ to CZNN (4), the FP-RFTZNN model is obtained:

$$\begin{aligned} & A^T \dot{X}B + B^T \dot{X}A \\ &= -\dot{A}^T X B - A^T X \dot{B} - \dot{B}^T X A \\ & \quad - B^T X \dot{A} - \dot{C} - \gamma F(A^T X B + B^T X A + C) \end{aligned} \quad (5)$$

in which $\gamma > 0$, and $F(\cdot)$ is a function array:

$$F(q) = (f(q_1), f(q_2), \dots, f(q_n))^T$$

where $q = (q_1, q_2, \dots, q_n)^T$, and

$$f(q_i) = q_i + \text{sign}(q_i)|q_i|^r, \quad i = 1, 2, \dots, n \quad (6)$$

where r is a real constant with $0 < r < 1$, and $\text{sign}(q_i)$ is a function returning the sign of the input value q_i .

When using circuits to realize neural networks, analog circuit components are prone to produce high-order residual errors. In addition, it is not surprising that truncation

or rounding errors occur in digital implementation. Model implementation errors eventually appear because of these facts [30]. Taken differential error $\Delta_A(t)$, $\Delta_B(t)$, $\Delta_C(t)$, and hardware implementation error $\Delta_H(t)$ into consideration, perturbed FP-RFTZNN model is obtained as follows:

$$\begin{aligned} & A^T \dot{X}B + B^T \dot{X}A \\ &= -(\dot{A} + \Delta_A)^T X B - A^T X (\dot{B} + \Delta_B) \\ & \quad - (\dot{B} + \Delta_B)^T X A - B^T X (\dot{A} + \Delta_A) - (\dot{C} + \Delta_C) \\ & \quad - \gamma F(A^T X B + B^T X A + C) + \Delta_H. \end{aligned} \quad (7)$$

Because $E(t) = A^T(t)X(t)B(t) + B^T(t)X(t)A(t) + C(t)$, perturbed FP-RFTZNN (7) is reformulated as

$$\begin{aligned} \dot{E}(t) = & -\gamma F(E(t)) - \Delta_A^T X B - A^T X \Delta_B - \Delta_B^T X A \\ & - B^T X \Delta_A - \Delta_C + \Delta_H \end{aligned}$$

which is equivalent to

$$\begin{aligned} \dot{e}(t) = & -\gamma F(e(t)) - \Delta_M(t)M^{-1}(t)e(t) \\ & + \Delta_M(t)M^{-1}(t)c(t) + (\Delta_h(t) - \Delta_c(t)) \end{aligned}$$

where $e(t) = \text{vec}(E(t))$; $\Delta_h(t) = \text{vec}(\Delta_H(t))$; $\Delta_c(t) = \text{vec}(\Delta_C(t))$; $\Delta_M(t) = B^T \otimes \Delta_A^T + \Delta_B^T \otimes A^T + A^T \otimes \Delta_B^T + \Delta_A^T \otimes B^T$; and, $M(t)$ and $x(t)$ are defined as before.

Set $R(t) = -\Delta_M(t)M^{-1}(t)$ and $r(t) = -R(t)c(t) + \Delta_h(t) - \Delta_c(t)$, we have

$$\dot{e}(t) = -\gamma F(e(t)) + R(t)e(t) + r(t). \quad (8)$$

From the above process, the robustness of FP-RFTZNN (5) can be equivalently demonstrated by monitoring the solution of (8).

B. Theoretical Analysis

Because it has been proven in [16] that RFTZNN (5) is finite-time convergent, we simply state the theorem without giving a concrete proof to avoid repetition.

Theorem 1: Given dynamic matrices $A(t)$, $B(t)$, and $C(t)$, which are assumed to satisfy *Assumption 1*, the state solution $X(t)$ to FP-RFTZNN (5), originating from any initial state $X(0) \in \mathbb{R}^{n \times n}$, converges to the theoretical time-varying solution of (1) in finite time t_c with

$$t_c \leq \max \left\{ \frac{1}{(1-r)\gamma} \ln(|e^+(0)|^{1-r} + 1), \frac{1}{(1-r)\gamma} \ln(|e^-(0)|^{1-r} + 1) \right\}$$

where $e^+(0)$ and $e^-(0)$ respectively refer to the largest and smallest element of $e(0)$.

As to the robustness of FP-RFTZNN (5), the following theorem indicates the boundedness of its residual error.

Theorem 2: Given dynamic matrices $A(t)$, $B(t)$, and $C(t)$, which are assumed to satisfy *Assumption 1*, if $\|A(t)\|_F$, $\|B(t)\|_F$, $\|C(t)\|_F$, $\|\Delta_A(t)\|_F$, $\|\Delta_B(t)\|_F$, $\|\Delta_H(t) - \Delta_C(t)\|_F$, and $\|M^{-1}(t)\|_F$ are, respectively, upper bounded by ϵ_A , ϵ_B , ϵ_C , δ_A , δ_B , δ_C , and ϕ , and $\gamma > 2\phi\epsilon_1/\rho$, then

$$\lim_{t \rightarrow +\infty} \|X(t) - X^*(t)\|_F \leq \frac{n(n+1)\epsilon_2\phi}{2(\gamma\rho - 2\phi\epsilon_1)}$$

validates for neural state $X(t)$ of perturbed FP-RFTZNN (7) originating from any initial state $X(0)$. Here, $\epsilon_1 = \delta_A \epsilon_B + \epsilon_A \delta_B$, $\epsilon_2 = 2\phi \epsilon_1 \epsilon_C + \delta_C$, and $\rho = f(|e_i|)/|e_i| > 1$.

Proof: Considering (8), a Lyapunov function $v = \|e(t)\|_2^2/2 \geq 0$ is defined in advance to facilitate the subsequent analysis of convergence. The time derivative of v along the solution to (8) is computed as

$$\begin{aligned} \dot{v} &= e^T \dot{e} = e^T (-\gamma f(e) + \text{Re} + r) \\ &= -\gamma e^T f(e) + e^T \text{Re} + e^T r. \end{aligned} \quad (9)$$

Evidently, the first term of (9) satisfies

$$-\gamma e^T f(e) = -\sum_{i=1}^{n^2} \gamma |e_i| f(|e_i|).$$

As to the second term of (9), we have $e^T \text{Re} \leq \|e\|_2 \|\text{Re}\|_2 \leq \|e\|_2^2 \|R\|_F = e^T e \|R\|_F$. The first inequality sign comes from the Cauchy inequality, and the second inequality sign results from the consistency between the induced 2-norm and Frobenius-norm of a matrix. Besides

$$\begin{aligned} \|R\|_F &= \|\Delta_M M^{-1}\|_F \leq \phi \|\Delta_M\|_F \\ &\leq \phi \|B^T \otimes \Delta_A^T + \Delta_B^T \otimes A^T + A^T \otimes \Delta_B^T + \Delta_A^T \otimes B^T\|_F \\ &\leq 2\phi (\|B\|_F \|\Delta_A\|_F + \|\Delta_B\|_F \|A\|_F) \\ &\leq 2\phi (\delta_A \epsilon_B + \epsilon_A \delta_B) := 2\phi \epsilon_1. \end{aligned}$$

For the last term of (9), $e^T r \leq \|e\|_2 \|r\|_2 \leq \|e\|_1 \|r\|_2$. Besides

$$\begin{aligned} \|r\|_2 &= \|-Rc + \Delta_h - \Delta_c\|_2 \leq \|Rc\|_2 + \|\Delta_h - \Delta_c\|_2 \\ &\leq \|R\|_F \|c\|_2 + \|\Delta_h - \Delta_c\|_2 \\ &= \|R\|_F \|C\|_F + \|\Delta_H - \Delta_C\|_F \\ &\leq 2\phi \epsilon_1 \epsilon_C + \delta_C := \epsilon_2. \end{aligned}$$

As a result

$$\begin{aligned} \dot{v} &\leq -\sum_{i=1}^{n^2} \gamma |e_i| f(|e_i|) + 2\phi \epsilon_1 e^T e + \epsilon_2 \|e\|_1 \\ &= -\sum_{i=1}^{n^2} |e_i| (\gamma f(|e_i|) - 2\phi \epsilon_1 |e_i| - \epsilon_2). \end{aligned} \quad (10)$$

Because inequality (10) has a similar form to inequality of (25), it is natural to infer that there is a similar conclusion for $\|e(t)\|_2$. That is, $\|e(t)\|_2$ is bounded.

In fact, inequality (10) can be reformulated as

$$\begin{aligned} \dot{v} &\leq -\sum_{i=1}^{n^2} |e_i| (\gamma f(|e_i|) - 2\phi \epsilon_1 |e_i| - \epsilon_2) \\ &= -\sum_{i=1}^{n^2} |e_i| (\gamma \rho |e_i| - 2\phi \epsilon_1 |e_i| - \epsilon_2) \\ &= -(\gamma \rho - 2\phi \epsilon_1) \sum_{i=1}^{n^2} |e_i| \left(|e_i| - \frac{\epsilon_2}{\gamma \rho - 2\phi \epsilon_1} \right) \end{aligned}$$

where there exists a sensitive parameter $\rho = f(|e_i|)/|e_i| > 1$.

By analyzing the last formula, we can easily find that when

$$|e_i| = \frac{\epsilon_2}{2(\gamma \rho - 2\phi \epsilon_1)}, \quad i \in \{1, \dots, n^2\}$$

the i th term of the last formula can achieve its highest value.

Set the values of all terms except the i th term as the maximum they can reach. For any $i \in \{1, 2, \dots, n^2\}$, we have

$$\dot{v} \leq -(\gamma \rho - 2\phi \epsilon_1) \left(|e_i|^2 - \frac{\epsilon_2}{\gamma \rho - 2\phi \epsilon_1} |e_i| - \frac{(n^2 - 1)\epsilon_2^2}{4(\gamma \rho - 2\phi \epsilon_1)^2} \right). \quad (11)$$

We denote

$$Z(|e_i|) = |e_i|^2 - \frac{\epsilon_2}{\gamma \rho - 2\phi \epsilon_1} |e_i| - \frac{(n^2 - 1)\epsilon_2^2}{4(\gamma \rho - 2\phi \epsilon_1)^2}$$

then the solution of $Z(|e_i|) = 0$ is

$$|e_i| = \frac{(n+1)\epsilon_2}{2(\gamma \rho - 2\phi \epsilon_1)}.$$

This leads to

$$\max_{1 \leq i \leq n^2} |e_i(t)| \leq \frac{(n+1)\epsilon_2}{2(\gamma \rho - 2\phi \epsilon_1)} \quad (12)$$

for sufficiently large t . If not, there exists $k \in \{1, 2, \dots, n^2\}$, such that $|e_k(t)|$ goes beyond that upper bound in inequality (12). Considering the graph of $Z(|e_i|)$ and (11), it can be deduced that $\dot{v} \leq 0$, which forces $\|e(t)\|_2$ to decrease. Accordingly, $\|e(t)\|_2$ will keep decreasing until $|e_k(t)|$ satisfies the inequality (12). Thus, inequality (12) validates.

Further, we obtain

$$\lim_{t \rightarrow +\infty} \|E(t)\|_F \leq \lim_{t \rightarrow +\infty} n \max_{1 \leq i \leq n^2} |e_i(t)| \leq \frac{n(n+1)\epsilon_2}{2(\gamma \rho - 2\phi \epsilon_1)}.$$

Because $\|X(t) - X^*(t)\|_F = \|M^{-1}(t)e(t)\|_2$, we have

$$\lim_{t \rightarrow +\infty} \|X(t) - X^*(t)\|_F \leq \lim_{t \rightarrow +\infty} \varphi \|e(t)\|_2 \leq \frac{n(n+1)\epsilon_2 \phi}{2(\gamma \rho - 2\phi \epsilon_1)}.$$

The proof of *Theorem 2* is now completed. \blacksquare

IV. VP-RFTZNN MODEL

It is unpractical for users to adjust the parameters at every turn to meet different requirements on accuracy and convergence time. An exponential-type varying-parameter $\gamma \exp(t)$ is thus employed to achieve faster convergence and better robustness. Based on this, VP-RFTZNN for solving DGLE is established, as well as its perturbed model. As proved, VP-RFTZNN has great advantages in terms of convergence and robustness: when perturbations do not exist, it converges faster than FP-RFTZNN; when perturbations exist, it still converges.

A. Design of VP-RFTZNN and Its Perturbed Version

Because of the similarity to the aforementioned FP-RFTZNN model, we directly present the VP-RFTZNN model as follows:

$$\begin{aligned} A^T \dot{X} B + B^T \dot{X} A &= -\dot{A}^T X B - A^T X \dot{B} - \dot{B}^T X A - B^T X \dot{A} \\ &\quad - \dot{C} - \gamma \exp(t) F (A^T X B + B^T X A + C). \end{aligned} \quad (13)$$

Analogous to Section III-A, the perturbed VP-RFTZNN can be designed as follows:

$$\begin{aligned} & A^T \dot{X} B + B^T \dot{X} A \\ &= -(\dot{A} + \Delta_A)^T X B - A^T X (\dot{B} + \Delta_B) \\ &\quad -(\dot{B} + \Delta_B)^T X A - B^T X (\dot{A} + \Delta_A) - (\dot{C} + \Delta_C) \\ &\quad -\gamma \exp(t) F(A^T X B + B^T X A + C) + \Delta_H \end{aligned} \quad (14)$$

which can be reformulated as

$$\dot{e}(t) = -\gamma \exp(t) F(e(t)) + R(t)e(t) + r(t) \quad (15)$$

where $\Delta_A, \Delta_B, \Delta_C, \Delta_H, R(t)$, and $r(t)$ are defined as in the previous section.

Remark 1: By the method of vectorization and simple mathematical transformations, we can transform VP-CFTZNN (13), which is established in matrix manner, into an explicit dynamic equation showing the relationship between the neurons. And then, the circuit diagram of this model can clearly show the realizability of VP-RFTZNN (13).

- 1) At first, vectorizing VP-RFTZNN (13) leads to

$$\begin{aligned} M(t)\dot{x}(t) &= -\dot{M}(t)x(t) - \dot{c}(t) - \gamma \exp(t) \\ &\quad \cdot F(M(t)x(t) + c(t)) \end{aligned}$$

where $M(t)$ is defined as before, $x(t) = \text{vec}(X(t)) \in \mathbb{R}^{n^2 \times 1}$, and $c(t) = \text{vec}(C(t)) \in \mathbb{R}^{n^2 \times 1}$.

- 2) Next, rewrite it as

$$\begin{aligned} \dot{x}(t) &= (M(t) + I)\dot{x}(t) + \dot{M}(t)x(t) + \dot{c}(t) + \gamma \exp(t) \\ &\quad \cdot F(M(t)x(t) + c(t)) \end{aligned}$$

in which $I \in \mathbb{R}^{n^2 \times n^2}$ represents the identity matrix.

- 3) The evolution formula of the i th neuron can be formulated as

$$\begin{aligned} \dot{x}_i(t) &= \sum_{j=1}^{n^2} \tilde{m}_{ij} \dot{x}_j(t) + \sum_{j=1}^{n^2} \tilde{m}_{ij} x_j(t) + \dot{c}_i(t) \\ &\quad + \gamma \exp(t) f \left(\sum_{j=1}^{n^2} m_{ij}(t) x_j(t) + c_i(t) \right). \end{aligned} \quad (16)$$

Here, we denote by $x_i(t)$ the value of the i th neuron at time instant t . For any vector v , we denote the i th element by v_i . For any matrix Y , we denote it by (y_{ij}) , where the subscript ij refers to the element at row i and column j . Here, $M(t) + I = (\tilde{m}_{ij}(t))$, $\dot{M}(t) = (\dot{\tilde{m}}_{ij}(t))$, and $M(t) = (m_{ij}(t))$.

Now, we can show the circuit implementation of our VP-RFTZNN (13) according to (16) as in Fig. 1.

Remark 2: As in Fig. 1, a separate processor is required to handle the nonlinear AF. Li and Li [32] have depicted the detailed hardware realization of the typical SBP-AF with analog devices, including diodes, amplifiers, etc. This also indicates that SSBP-AF (6) is realizable with analog devices. We omit the specific realization because of the similarity between the typical SBP function and SSBP-AF (6).

B. Theoretical Analysis

In this section, theoretical analyses are conducted to prove the finite-time convergence of VP-RFTZNN (13). In addition, perturbed VP-RFTZNN (14) is proven to converge as time tends to positive infinity. More definite expressions, concerning the upper and lower bounds for the residual error, as well as the specific time it takes to start decreasing monotonically and super-exponentially, are estimated quantitatively.

Theorem 3: Given dynamic matrices $A(t)$, $B(t)$, and $C(t)$, which is assumed to satisfy *Assumption 1*, the state solution $X(t)$ of VP-RFTZNN (13), originating from any initial state $X(0) \in \mathbb{R}^{n \times n}$, converges to the theoretical time-varying solution to (1) in finite time t_c :

$$t_c \leq \max \left\{ \ln \left(\frac{1}{(1-r)\gamma} \ln(|e^+(0)|^{1-r} + 1) + 1 \right), \ln \left(\frac{1}{(1-r)\gamma} \ln(|e^-(0)|^{1-r} + 1) + 1 \right) \right\}$$

in which $e^+(0)$ and $e^-(t)$ are defined as in *Theorem 1*.

Proof: At first, we assumed that $e^+(0) \geq e_i(0)$ and $e^-(0) \leq e_i(0)$, $i \in \{1, 2, \dots, n^2\}$. Note that the time derivative of every element in $e(t)$ has the same expression; we conclude that $e^+(t) \geq e_i(t)$ and $e^-(t) \leq e_i(t)$, $\forall t \geq 0$, $i \in \{1, 2, \dots, n^2\}$. Hence, If $e^+(t_c) = 0$ and $e^-(t_c) = 0$ for $t_c < +\infty$, every element $e_i(t)$ in $e(t)$ converges to 0 within finite time.

Besides, the vector form of the error function satisfies $\dot{e}(t) = -\gamma \exp(t) F(e(t))$, which leads to

$$\dot{e}_i(t) = -\gamma \exp(t) (e_i(t) + \text{sign}(e_i(t)) |e_i(t)|^r). \quad (17)$$

It is clear that $\dot{e}_i(t)$ has the opposite sign from $e_i(t)$. Hence, $e_i(t)$ decreases monotonically and keeps nonnegative when $e_i(0) \geq 0$, and increases monotonically but still keeps nonpositive when $e_i(0) \leq 0$. This implies that once $e_i(t)$ reaches 0, it will maintain this stable state. Namely, $\forall t \geq t_c$, $e^+(t) = 0$ and $e^-(t) = 0$ hold true.

Next, we only focus on the case of $e^+(t)$, because $e^-(t)$ can be certificated through the same arguments. Specifically, the convergence of $e^+(t)$ will be divided into the following three cases according to the sign of $e^+(0)$:

- 1) When $e^+(0) > 0$, we have

$$\dot{e}^+(t) = -\gamma \exp(t) (e^+(t) + (e^+(t))^r)$$

which can be further rewritten as

$$\frac{d(e^+(t))}{e^+(t) + (e^+(t))^r} = -\gamma \exp(t) dt. \quad (18)$$

Supposing that there exists $t_f^+ \geq 0$ such that $e^+(t_f^+) = 0$, integrating (18) from 0 to t_f^+ results

$$\int_{e^+(0)}^{e^+(t_f^+)} \frac{d(e^+(t))}{e^+(t) + (e^+(t))^r} = \int_0^{t_f^+} -\gamma \exp(t) dt$$

from which the following result is obtained:

$$\frac{1}{1-r} \ln \left((e^+(t))^{1-r} + 1 \right) \Big|_{e^+(0)}^{t_f^+} = -\gamma \exp(t) \Big|_0^{t_f^+}.$$

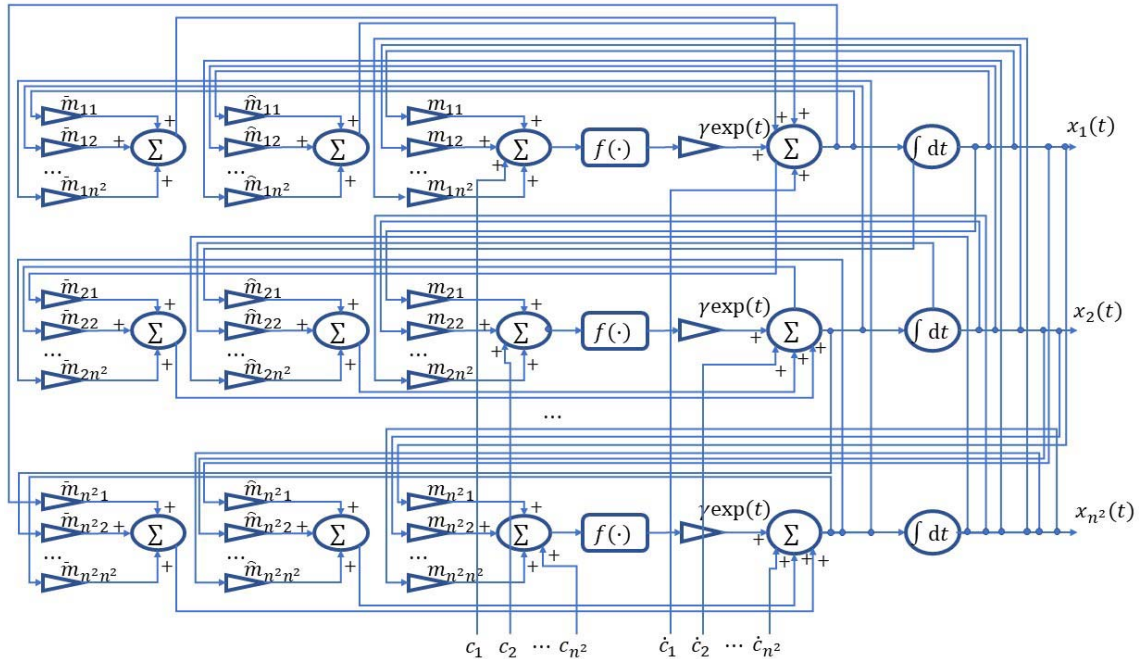


Fig. 1. Circuit schematic for VP-RFTZNN (13).

That is,

$$\frac{1}{1-r} \ln \frac{1}{(e^+(0))^{1-r} + 1} = -\gamma \exp(t_f^+) + \gamma.$$

Hence, we can solve t_f^+ as

$$t_f^+ = \ln \left(\frac{1}{(1-r)\gamma} \ln \left((e^+(0))^{1-r} + 1 \right) + 1 \right).$$

2) When $e^+(0) < 0$, we have

$$\dot{e}^+(t) = -\gamma \exp(t)(e^+(t) - (e^+(t))^r)$$

which can be further rewritten as

$$\frac{d(e^+(t))}{e^+(t) - (e^+(t))^r} = -\gamma \exp(t) dt.$$

Recall that if $e^+(0) < 0$, we have $e^+(t) \leq 0, \forall t \geq 0$. Hence, $-|e^+(t)| = e^+(t)$ validates for all nonnegative t , which leads to

$$\frac{-d(|e^+(t)|)}{-|e^+(t)| - |e^+(t)|^r} = -\gamma \exp(t) dt.$$

That is,

$$\frac{d(|e^+(t)|)}{|e^+(t)| + |e^+(t)|^r} = -\gamma \exp(t) dt$$

which has a similar form of (18). Consequently, after analogous procedures, t_f^+ can be calculated as

$$t_f^+ = \ln \left(\frac{1}{(1-r)\gamma} \ln \left(|e^+(0)|^{1-r} + 1 \right) + 1 \right).$$

3) When $e^+(0) = 0$, it is evident that 0 is lower than the UB-CT t_f^+ .

To sum up the above three cases for $e^+(t)$, the UB-CT t_f^+ can be estimated as

$$t_f^+ = \ln \left(\frac{1}{(1-r)\gamma} \ln \left(|e^+(0)|^{1-r} + 1 \right) + 1 \right).$$

Similarly, we can also deduce the UB-CT t_f^- for the situation of $e^-(t)$

$$t_f^- = \ln \left(\frac{1}{(1-r)\gamma} \ln \left(|e^-(0)|^{1-r} + 1 \right) + 1 \right).$$

As a result, the UB-CT for the VP-RFTZNN (13) is derived as

$$t_c \leq \max \left\{ \ln \left(\frac{1}{(1-r)\gamma} \ln \left(|e^+(0)|^{1-r} + 1 \right) + 1 \right), \ln \left(\frac{1}{(1-r)\gamma} \ln \left(|e^-(0)|^{1-r} + 1 \right) + 1 \right) \right\}.$$

Evidently, VP-RFTZNN (13) achieves a faster convergence rate than FP-RFTZNN (5) according to the inequality $\ln(1+x) < x$ when $x > 0$. As to the robustness, the following two theorems reveal the great advantage of VP-RFTZNN (13) through analyzing the convergence of perturbed VP-RFTZNN (14).

Theorem 4: With ρ , ϕ , and ϵ_1 defined in *Theorem 2*, assuming that $\gamma \rho \exp(t) > 2\phi\epsilon_1$, residual error $\|E(t)\|_F$ of perturbed VP-RFTZNN (14) decreases to 0 as time evolves, which indicates that the solution of VP-RFTZNN (14) converges to the theoretical solution of (1).

Proof: Analogous to *Theorem 2*, an upper bound for the residual error $\|E(t)\|_F$ can be derived as

$$\|E(t)\|_F \leq \frac{n(n+1)\epsilon_2}{2(\gamma \exp(t)\rho - 2\phi\epsilon_1)} := \bar{w}(t).$$

This leads to the fact that $\lim_{t \rightarrow +\infty} \|E(t)\|_F = 0$ and $\lim_{t \rightarrow +\infty} \|X(t) - X^*(t)\|_F = 0$, which completes the proof. ■

Remark 3: Because of the monotonicity of varying parameter $\gamma \exp(t)$, it takes finite time $\bar{t} = \ln((2\phi\epsilon_1)/(\gamma\rho))$ to achieve $\gamma\rho \exp(t) > 2\phi\epsilon_1$. Hence, starting from $X(\bar{t})$, the solution of perturbed VP-RFTZNN (14) converges to the theoretical state $X^*(t)$. That is, the requirement on parameter as described in *Theorem 4* is in fact nothing. The global convergence and unconstrained parameter show the significant advantage of perturbed VP-RFTZNN (14) over perturbed FP-RFTZNN (7), indicating the great superiority of VP-RFTZNN (13) over FP-RFTZNN (5).

It is noted that the uniform boundedness of coefficient matrices and perturbation matrices in *Theorem 2* and *Theorem 4* are too strong. In reality, this is necessary for FP-RFTZNN (5), but not for VP-RFTZNN (13). When it comes to linear perturbation matrices, ϵ_1 and ϵ_2 , which used to be two constants, grow linearly with time t . For *Theorem 2*, the upper bound of residual error converges to $+\infty$. For *Theorem 4*, the exponential item $\gamma \exp(t)\rho$ grows much faster than any polynomial function, and thus VP-RFTZNN (13) still converges. The following corollary illustrates this view.

Corollary 1: Suppose that the Frobenius norms mentioned in *Theorem 2* are bounded but not uniformly bounded, which means $\epsilon_A = \epsilon_A(t)$, $\epsilon_B = \epsilon_B(t)$, $\epsilon_C = \epsilon_C(t)$, $\phi = \phi(t)$, $\delta_A = \delta_A(t)$, $\delta_B = \delta_B(t)$, and $\delta_C = \delta_C(t)$. The neural state $X(t)$ of VP-RFTZNN (13) will converge to $X^*(t)$ if

$$\lim_{t \rightarrow +\infty} \frac{n(n+1)\phi(t)\epsilon_2(t)}{2\gamma \exp(t)\rho - 4\phi(t)\epsilon_1(t)} = 0$$

where $\epsilon_1(t)$ and $\epsilon_2(t)$ are defined as in *Theorem 2*.

Remark 4: According to *Corollary 1*, it can be deduced that VP-RFTZNN (13) still converges when upper bounds of corresponding matrices are polynomial functions. However, the convergence might be very slow. Hence, it is wise to choose an appropriate parameter γ making $\gamma \exp(t)\rho > 2\phi(t)\epsilon_1(t)$ valid for any $t \geq 0$. For example, suppose that $2\phi(t)\epsilon_1(t) = \sum_{i=0}^p a_i t^i$, γ satisfying $\gamma > \max_{0 \leq j \leq p} \{j!a_j\}/\rho$ would be a good choice.

Theorem 5: Under the same conditions as *Theorem 4*, after a period time of $t_1 \geq 0$, the residual error $\|E(t)\|_F$ of perturbed VP-RFTZNN (14) will either monotonically decrease to the interval $[0, \underline{w}(t)]$ at a super-exponential convergence rate $s(t)$ in a finite time and stay within this interval all time, or monotonically decrease to 0 with a super-exponential convergence rate $s(t)$ and stay within the interval $[\underline{w}(t), \overline{w}(t)]$ all time. The involved unknown parameters are derived as

$$t_1 = \ln \frac{4\phi\epsilon_1 + \sqrt{2n}\epsilon_2}{2\gamma + (\sqrt{2s_1})^{1+r} \gamma}$$

$$s(t) = \frac{(1-\alpha)(g_2(t) - g_2(t_2))}{2(t-t_2)}$$

$$\underline{w}(t) = \frac{2n\epsilon_2}{\alpha \left(2\gamma \exp(t) + (\sqrt{2s_1})^{r+1} \gamma \exp(t) - 4\phi\epsilon_1 \right)}$$

among which $s_1 > 0$ and $0 < \alpha < 1$ are positive constants, and

$$g_1(t) = \left(2 + (\sqrt{2s_1})^{r+1} \right) \gamma \exp(t) - (4\phi\epsilon_1 + \sqrt{2n}\epsilon_2)t$$

$$g_2(t) = \left(2 + (\sqrt{2s_1})^{r+1} \right) \gamma \exp(t) - 4\phi\epsilon_1 t$$

$$t_2 = h_1 \left(g_1(t_1) - 2 + 2\sqrt{v(t_1)} \right)$$

where $h_1(\cdot)$ is the inverse function of $g_1(\cdot)$.

Proof: Similar to *Theorem 2*, we define $v(t) = \|e(t)\|_2^2/2$ and can deduce that

$$\begin{aligned} \dot{v}(t) &\leq -\gamma \exp(t) (\|e(t)\|_2^2 + \|e(t)\|_{r+1}^{r+1}) + 2\phi\epsilon_1 \|e(t)\|_2^2 \\ &\quad + \epsilon_2 \|e(t)\|_1 \\ &\leq -\gamma \exp(t) (\|e(t)\|_2^2 + (s_1 \|e(t)\|_2)^{r+1}) + 2\phi\epsilon_1 \|e(t)\|_2^2 \\ &\quad + n\epsilon_2 \|e(t)\|_2 \\ &\leq -\gamma \exp(t) \left(2v(t) + s_1^{r+1} (2v(t))^{\frac{r+1}{2}} \right) + 4\phi\epsilon_1 v(t) \\ &\quad + n\epsilon_2 \sqrt{2v(t)} \\ &= -(2\gamma \exp(t) - 4\phi\epsilon_1)v(t) - \left(\sqrt{2s_1} \right)^{r+1} \gamma \exp(t) \\ &\quad \cdot (v(t))^{\frac{r+1}{2}} + \sqrt{2n}\epsilon_2 (v(t))^{\frac{1}{2}}. \end{aligned}$$

The second inequality comes from the fact that $\|u\|_2 \leq \|u\|_1 \leq n\|u\|_2$ and $s_1 \|u\|_2 \leq \|u\|_{r+1} \leq s_2 \|u\|_2$ for any $u \in \mathbb{R}^{n^r \times 1}$, in which s_1 and s_2 are positive constants. We claim that such constants exist because of the equivalence of norms.

When $t \geq t_1$, we have $\dot{g}_1(t) \geq 0$ and $\dot{g}_2(t) \geq 0$. According to the result in *Theorem 4*, it is clear that $\lim_{t \rightarrow +\infty} v(t) = 0$. Therefore, if $v(t_1) \geq 1$, there exists $t_2 \geq t_1$ such that $v(t) \geq 1$ validates for any $t \in [t_1, t_2]$ and $v(t_2) = 1$. In this case, $v(t) \geq (v(t))^{(1+r)/2} \geq (v(t))^{1/2}$ for any $t \in [t_1, t_2]$. Hence,

$$\begin{aligned} \dot{v} &\leq -(2\gamma \exp(t) - 4\phi\epsilon_1)v^{\frac{1}{2}} - \left(\sqrt{2s_1} \right)^{r+1} \gamma \exp(t)v^{\frac{1}{2}} \\ &\quad + \sqrt{2n}\epsilon_2 v^{\frac{1}{2}} = -\dot{g}_1(t)v^{\frac{1}{2}} \leq 0. \end{aligned}$$

Integrating both sides of inequality $\dot{v}(t) \leq -\dot{g}_1(t)(v(t))^{1/2}$ from t_1 to t_2 , we have

$$2 - 2\sqrt{v(t_1)} \leq g_1(t_1) - g_1(t_2).$$

Because $\dot{g}_1(t) > 0$ validates for any $t > t_1$, $g_1(t)$ monotonically increases in the interval $[t_1, t_2]$. The inverse function $t = h_1(y)$ exists and monotonically increases in the interval $[t_1, t_2]$. Thus,

$$t_2 \leq h_1 \left(g_1(t_1) - 2 + 2\sqrt{v(t_1)} \right).$$

Here, we have to note that, if

$$\gamma \geq \frac{4\phi\epsilon_1 + \sqrt{2n}\epsilon_2}{2 + (\sqrt{2s_1})^{r+1}} := \gamma_0$$

then, $t_1 = 0$ and

$$t_2 = h_1 \left(\left(2\gamma + (\sqrt{2s_1})^{r+1} \right) \gamma - 2 + 2\sqrt{v(0)} \right).$$

Now, we have proved that after a period of time t_1 , if $v(t_1) \geq 1$, $v(t)$ will monotonically decrease to 1 within a finite

time of $t_2 - t_1$. Especially, in the case of $\gamma \geq \gamma_0$, if $v(0) \geq 1$, $v(t)$ will monotonically decrease to 1 within a finite time of t_2 .

For the case of $v(t_1) < 1$, we let $t_2 = t_1$. Then $v(t_2) \leq 1$. Now, we only have to discuss the case of $t \geq t_2$.

We claim that $v(t) \leq 1$ validates for any $t \in [t_2, +\infty)$. If not, there exists $\tilde{t} > t_2$, such that $v(\tilde{t}) > 1$. Set $t_3 = \max\{t \in [t_2, \tilde{t}] | v(t) = 1\}$, for $t \in (t_3, \tilde{t}]$, it is clear that $v(t) > 1$. However, according to the previous analysis, $\dot{v}(t_3) < 0$. This leads to a contradiction.

In this situation, $v(t) \leq (v(t))^{(r+1)/2} \leq v(t)^{1/2}$ and

$$\begin{aligned} \dot{v} &\leq -(2\gamma \exp(t) - 4\phi\epsilon_1)v - \left(\sqrt{2}s_1\right)^{r+1} \gamma \exp(t)v \\ &\quad + \sqrt{2n}\epsilon_2 v^{1/2} \\ &= -\dot{g}_2(t)v + \sqrt{2n}\epsilon_2 v^{1/2} \\ &= -(1-\alpha)\dot{g}_2(t)v - \left(\alpha\dot{g}_2(t)v - \sqrt{2n}\epsilon_2 v^{1/2}\right). \end{aligned}$$

One sufficient condition for $\dot{v}(t) \leq 0$ to be valid is

$$\alpha\dot{g}_2(t)v(t) \geq \sqrt{2n}\epsilon_2(v(t))^{1/2}.$$

That is,

$$(v(t))^{1/2} \geq \frac{\sqrt{2n}\epsilon_2}{\alpha\dot{g}_2(t)}$$

which leads to $\|e(t)\|_2 \geq \underline{w}(t)$.

When $\|e(t)\|_2 \geq \underline{w}(t)$, we have

$$\dot{v}(t) \leq -(1-\alpha)\dot{g}_2(t)v(t).$$

According to the theory of ordinary differential equations as well as the comparison theorem, it is evident that

$$v(t) \leq v(t_2) \exp(-(1-\alpha)(g_2(t) - g_2(t_2))).$$

As a result

$$\|e(t)\|_2 \leq \|e(t_2)\|_2 \exp\left(\frac{-(1-\alpha)(g_2(t) - g_2(t_2))}{2}\right).$$

This means, once the residual error $\|E(t)\|_F$ exceeds $\underline{w}(t)$, it will monotonically decrease to the interval $[0, \underline{w}(t)]$ with an exponential convergence rate

$$s(t) = \frac{(1-\alpha)(g_2(t) - g_2(t_2))}{2(t-t_2)}.$$

We call it super-exponential convergent because $\lim_{t \rightarrow +\infty} s(t) = +\infty$. If it takes $t_c \in [t_2, +\infty)$ for $\|E(t)\|_F$ to converge to the interval $[0, \underline{w}(t)]$, it will stay in this interval all time after the convergence. Or else, with a super-exponential convergence rate, the residual error $\|E(t)\|_F$ will decrease to 0 monotonically and infinitely, and it keeps in the interval $[\underline{w}(t), \bar{w}(t)]$ after a finite time. The proof is completed. ■

Theorem 5 further demonstrates the monotonicity and super-exponential convergence of perturbed VP-RFTZNN (14) and shows quantitatively estimated expressions concerning the bounds for the error state and the time it takes to start decreasing monotonically and super-exponentially.

V. COMPARISON VERIFICATION

With above theoretical analyses, VP-RFTZNN (13) is verified to be superior to FP-RFTZNN (5) in terms of convergence and robustness when applied to solve (1). In this section, an example of DGLE is elegantly constructed for verifying the superiority. Because of the strong robustness of PIDT-ZNN in [23] and [33], of which the design formula is

$$\dot{E}(t) = -\gamma \left(F(E(t)) + \int_0^t F(E(s)) ds \right) \quad (19)$$

it is also cited to solve the example as a comparison. As seen, the same nonlinear AF as models (5) and (13) is applied to PIDT-ZNN (19) to make sure the comparison is fair. In the end, a robot manipulator with four degree of freedom (DOF) is shown and controlled by the method of VP-RFTZNN to draw a circle in 3-D Euclidean space. Relevant experiments are completed based on the ode45 solver of MATLAB.

A. Numerical Example

Based on the example of standard Lyapunov equation in [16], an example of DGLE is constructed as follows:

$$\begin{aligned} A(t) &= \begin{bmatrix} -1 - \frac{1}{2} \cos(2t) & \frac{1}{2} \sin(2t) \\ \frac{1}{2} \sin(2t) & -1 + \frac{1}{2} \cos(2t) \end{bmatrix} \\ B(t) &= \begin{bmatrix} \frac{2}{3} \cos(2t) - \frac{4}{3} & -\frac{2}{3} \sin(2t) \\ -\frac{2}{3} \sin(2t) & -\frac{2}{3} \cos(2t) - \frac{4}{3} \end{bmatrix} \\ C(t) &= \begin{bmatrix} -2 \cos(t) & \frac{10}{3} \sin(t) \\ -\frac{4}{3} \sin(t) & -2 \cos(t) \end{bmatrix} \\ X(t) &= \begin{bmatrix} \cos(t) - \sin(t) \\ \sin(t) \cos(t) \end{bmatrix}. \end{aligned}$$

Note that this constructed example is uniquely solvable and that the coefficient matrices are uniformly bounded. It is calculated that

$$\epsilon_A = \frac{\sqrt{10}}{2}, \quad \epsilon_B = \frac{2}{3}\sqrt{10}, \quad \epsilon_C = \frac{10}{3}\sqrt{2}, \quad \phi = \frac{\sqrt{17}}{5}.$$

To testify the robustness of two RFTZNN models, the following four kinds of perturbation matrices are considered:

- 1) Constant: $\Delta_A = \Delta_B = \Delta_H - \Delta_C \equiv 1/4E_2$.
- 2) Sinusoidal

$$\begin{aligned} \Delta_A &= \begin{bmatrix} \cos(t) & 0 \\ 0 & \sin(t) \end{bmatrix}, \quad \Delta_B = \begin{bmatrix} \sin(t) & 0 \\ 0 & \cos(t) \end{bmatrix} \\ \Delta_H - \Delta_C &= \begin{bmatrix} \sin(t) & 0 \\ 0 & -\cos(t) \end{bmatrix}. \end{aligned}$$

- 3) Linear: $\Delta_A = \Delta_B = \Delta_H - \Delta_C = 1/4tE_2$.
- 4) Quadratic: $\Delta_A = \Delta_B = \Delta_H - \Delta_C = 1/4t^2E_2$.

The first two groups of perturbation matrices satisfy the uniformly bounded condition required by *Theorem 2*, *Theorem 4*, and *Theorem 5*, whereas the last two do not. According to *Theorem 2*, to ensure the boundedness of residual error of FP-RFTZNN (5), γ should be larger than 3.0423 for the first

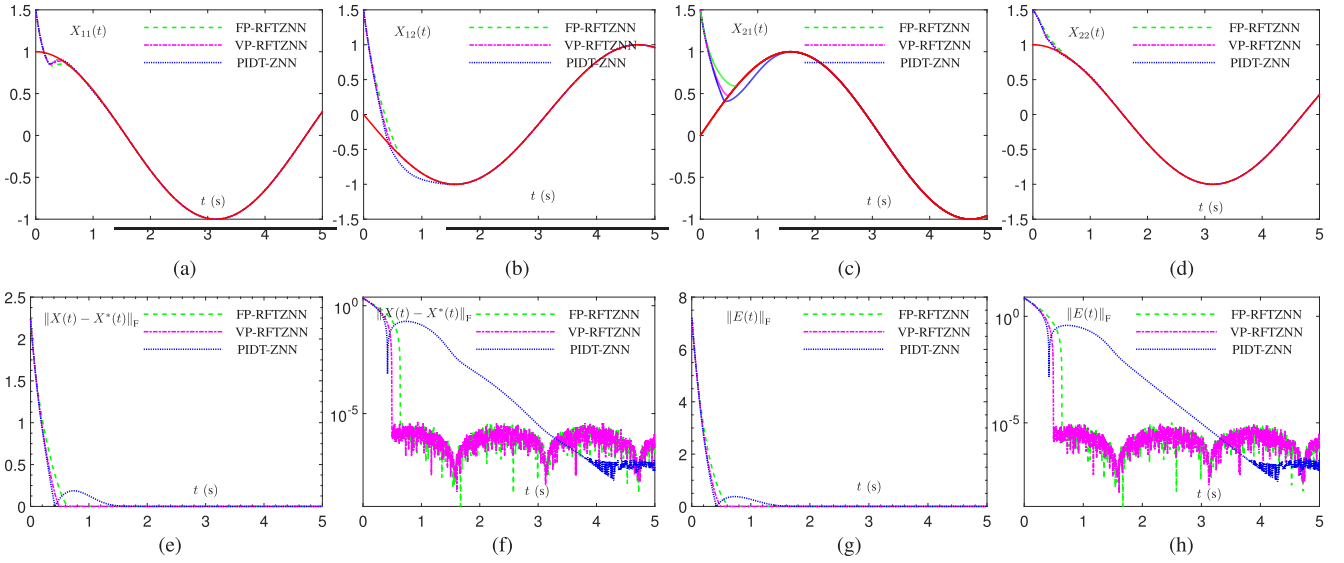


Fig. 2. Transient behaviors of FP-RFTZNN (5), VP-RFTZNN (13), and PIDT-ZNN (19) when applied to solve the example in Section V-A. The red solid curves correspond to the theoretical solution $X^*(t)$. (a) $X_{11}(t)$. (b) $X_{12}(t)$. (c) $X_{21}(t)$. (d) $X_{22}(t)$. (e) $\|X(t) - X^*(t)\|_F$. (f) $\|X(t) - X^*(t)\|_F$. (g) $\|E(t)\|_F$. (h) $\|E(t)\|_F$.

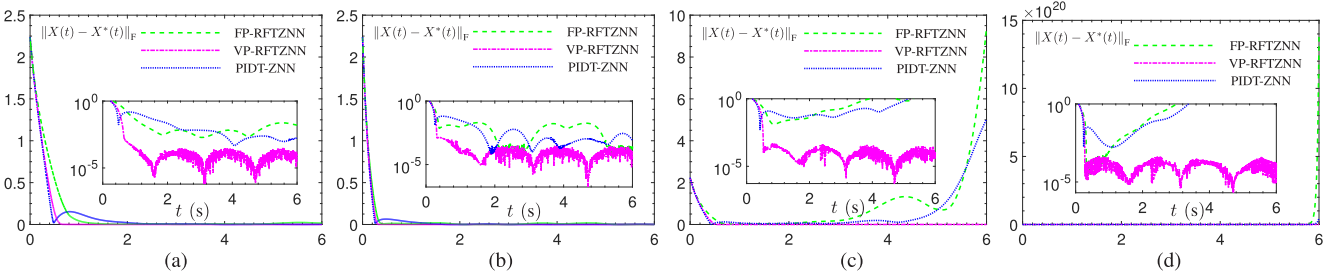


Fig. 3. Transient behaviors of FP-RFTZNN (5), VP-RFTZNN (13), and PIDT-ZNN (19) when applied to solve the example in Section V-A with four kinds of perturbation matrices are considered. (a) Constant. (b) Sinusoidal. (c) Linear. (d) Quadratic.

group of perturbation matrices and be larger than 6.0846 for the second group. As to the last two cases, the boundedness cannot be guaranteed. According to *Remark 3* and *Corollary 1*, VP-RFTZNN (13) is convergent for the four cases with any $\gamma > 0$. However, it is wise to set $\gamma > 3.0423$ for the constant case; $\gamma > 6.0846$ for the sinusoidal case; $\gamma > 3.0423$ for the linear case; and $\gamma > 6.0846$ for the quadratic case.

1) *Convergence*: Set $\gamma = 3$ and $X(0) = 1.5E_2$. Fig. 2 illustrates the convergence performance of two RFTZNN models when applied to solve this DGLE. As seen, PIDT-ZNN (19) is also experimented as a comparison. Noting that the relative tolerance and absolute tolerance are adjusted as 10^{-6} and 10^{-8} , respectively, we compare the convergence speed of the three models by observing the time when the error norms in Fig. 2(f) and (h) converge to 10^{-6} . It is evident that VP-RFTZNN (13) has the fastest convergence rate, followed by FP-RFTZNN (5) and PIDT-ZNN (19). Besides, the convergence curve of PIDT-ZNN (19) has obvious delay convergence property, which resulted from the integral item of its design formula. The factor contributing to the good robustness of PIDT-ZNN (19) also brings the model bad influence to the convergence. As observed in Fig. 2(h), the residual errors of FP-RFTZNN (5) and VP-RFTZNN (13) converge to 10^{-6} after about 0.63 s and 0.49 s, respectively. This observation

coincides with the deductions in *Theorem 1* and *Theorem 3*. Actually, it is easy to calculate the UBs-CT of two RFTZNN models as 0.6380 s and 0.4935 s, respectively.

2) *Robustness*: The initial state is set to $1.5E_2$, the relative tolerance is set to 10^{-4} , and the absolute tolerance is set to 10^{-6} . According to the analysis at the beginning of Section V-A, we set $\gamma = 3.1$ for the constant case; $\gamma = 6.1$ for the sinusoidal case; $\gamma = 3.1$ for the linear case; and $\gamma = 6.1$ for the quadratic case. As can be seen in Fig. 3, the solution error of VP-RFTZNN (13) monotonically converges to the level of 10^{-4} within less than 0.4 s for the four kinds of perturbation matrices, whereas that of FP-RFTZNN (5) is bounded only if the perturbation matrices are constant or sinusoidal. That is, the uniform boundedness of perturbation matrices is necessary for FP-RFTZNN model to realize its boundedness of solution error. In addition, VP-RFTZNN (13) can monotonically converge to a good accuracy in a short time, whereas PIDT-ZNN (19) that claims good robustness perform about as well over this time period as FP-RFTZNN (5) that converges only to a bounded interval.

B. Application to Robot Manipulator

A robot manipulator consisting of three revolute joints and one prismatic joint is shown in Fig. 4(a), and its

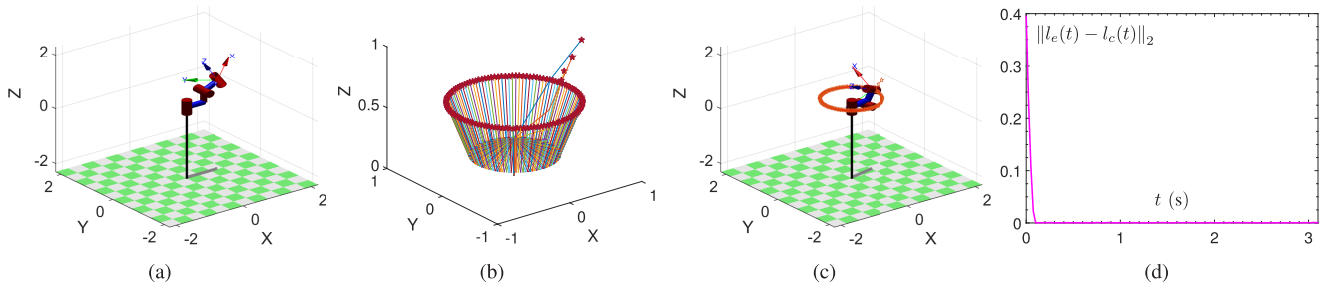


Fig. 4. Simulation performance of VP-RFTZNN (13) controlling a 4-DOF robot to draw a circle in 3-D Euclidean space. (a) Simulated appearance of the 4-DOF robot. (b) Joints position in motion, which is described by the origin of the joint coordinate system. (c) Phase of the moving robot. (d) Distance between the actual position and the desired position.

TABLE I
DH PARAMETER LIST

| i | α_{i-1} | a_{i-1} | d_i | θ_i |
|-----|----------------|-----------|-------|------------|
| 1 | 0 | 0 | 0.3 | p_1 |
| 2 | 0 | 0.5 | p_2 | 0 |
| 3 | $\pi/2$ | 0 | 0 | p_3 |
| 4 | $-\pi/2$ | 0.5 | 0 | p_4 |

Denavit-Hartenberg (DH) parameter list defined by the modified DH parameter method [34] is summarized in Table I, with p_1 , p_2 , p_3 , and p_4 representing the joint variables. Here the robot is controlled by VP-RFTZNN (13) to draw a circle in 3-D Euclidean space within 3.1 s, of which the coordinate is

$$l_c(t) = [0.75 \cos(2\pi t/3), 0.75 \sin(2\pi t/3), 0.6], \quad t \in [0, 3].$$

For convenience, the position of the end-effector is assumed to coincide with the origin of the fourth joint coordinate system. Evidently, the forward kinematic equation of the robot is

$$l_e(t) = \begin{bmatrix} 0.5 \cos p_1 \cos p_3 + 0.5 \cos p_1 \\ 0.5 \sin p_1 \cos p_3 + 0.5 \sin p_1 \\ 0.5 \sin p_3 + 0.3 + p_2 \end{bmatrix} := h(p(t))$$

where $p(t) = [p_1(t), p_2(t), p_3(t), p_4(t)]$. The control formulas based on VP-RFTZNN (13) are formulated as

$$\dot{p}(t) = J^+(p)(\dot{l}_c(t) + \gamma \exp(t)F(l_c - h(p(t))))$$

where $J(p)$ represents the Jacobian matrix of $h(p)$ with respect to p , and $J^+(p)$ represents the pseudo-inverse of $J(p)$. Set $\gamma = 3$ and $p(0) = [0, 0.4, \pi/6, \pi/3]$. Fig. 4(b)–(d) shows that the method based on VP-RFTZNN (13) can effectively control the robot to draw a curve that is very consistent with the target trajectory, and it takes only 0.1 s for the robot to follow the desired path.

VI. CONCLUSION

Based on the purpose of searching a more efficient approach to solve DGLE in real time, a new design formula with time-varying parameter was proposed and compared with the case of fixed parameter. Rigorous mathematical proof of convergence for VP-RFTZNN was presented and the UB-CT was

estimated to show its superiority to FP-RFTZNN. Then, their robustness were further proved by analyzing two perturbed RFTZNN models with differential errors and implementation errors. The convergence of perturbed VP-RFTZNN model was obtained, which indicated the superiority of VP-RFTZNN model to FP-RFTZNN model. Comparative simulations further certificated the efficacy and superiority of VP-RFTZNN model over FP-RFTZNN model when tackling DGLE online.

REFERENCES

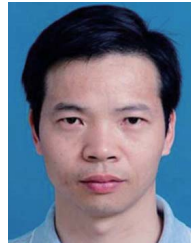
- [1] B. Zhou, G.-R. Duan, and Z. Lin, "A parametric periodic Lyapunov equation with application in semi-global stabilization of discrete-time periodic systems subject to actuator saturation," *Automatica*, vol. 47, no. 2, pp. 316–325, Feb. 2011.
- [2] H. Zhang, Z. Li, Z. Qu, and F. L. Lewis, "On constructing Lyapunov functions for multi-agent systems," *Automatica*, vol. 58, pp. 39–42, Aug. 2015.
- [3] P. Benner, "Solving large-scale control problems," *IEEE Control Syst.*, vol. 24, no. 1, pp. 44–59, Feb. 2004.
- [4] X. Yang, Z. Ding, J. Zhang, and S. Sun, "On the eigenvalue estimation for solution to Lyapunov equation," *Appl. Math. Comput.*, vol. 217, no. 16, pp. 6974–6980, Apr. 2011.
- [5] I. Mutlu, F. Schrödel, N. Bajcinca, D. Abel, and M. T. Söylemez, "Lyapunov equation based stability mapping approach: A MIMO case study," *IFAC-PapersOnLine*, vol. 49, no. 9, pp. 130–135, 2016.
- [6] Y. Zhang, W. E. Leithead, and D. J. Leith, "Time-series Gaussian process regression based on Toeplitz computation of $O(N^2)$ operations and $O(N)$ -level storage," in *Proc. 44th IEEE Conf. Decis. Control*, Dec. 2005, pp. 3711–3716.
- [7] F. Ding and T. Chen, "Gradient based iterative algorithms for solving a class of matrix equations," *IEEE Trans. Autom. Control*, vol. 50, no. 8, pp. 1216–1221, Aug. 2005.
- [8] F. Ding and H. Zhang, "Gradient-based iterative algorithm for a class of the coupled matrix equations related to control systems," *IET Control Theory Appl.*, vol. 8, no. 15, pp. 1588–1595, Oct. 2014.
- [9] C. Yi, Y. Chen, and Z. Lu, "Improved gradient-based neural networks for online solution of Lyapunov matrix equation," *Inf. Process. Lett.*, vol. 111, no. 16, pp. 780–786, Aug. 2011.
- [10] Y. Zhang, K. Chen, X. Li, C. Yi, and H. Zhu, "Simulink modeling and comparison of Zhang neural networks and gradient neural networks for time-varying Lyapunov equation solving," in *Proc. IEEE Int. Conf. Natur. Comput.*, vol. 3, Oct. 2008, pp. 521–525.
- [11] C. Yi, Y. Chen, and X. Lan, "Comparison on neural solvers for the Lyapunov matrix equation with stationary & nonstationary coefficients," *Appl. Math. Model.*, vol. 37, no. 4, pp. 2495–2502, 2013.
- [12] C. Aouiti, "Oscillation of impulsive neutraldelay generalized high-order Hopfield neural networks," *Neural Comput. Appl.*, vol. 29, no. 9, pp. 477–495, May 2018.
- [13] C. Aouiti and F. Dridi, "Piecewise asymptotically almost automorphic solutions for impulsive non-autonomous high-order hopfield neural networks with mixed delays," *Neural Comput. Appl.*, vol. 31, no. 9, pp. 5527–5545, Sep. 2019.
- [14] C. Aouiti, M. S. M'hamdi, and A. Touati, "Pseudo almost automorphic solutions of recurrent neural networks with time-varying coefficients and mixed delays," *Neural Process. Lett.*, vol. 45, pp. 121–140, Oct. 2017.

- [15] C. Aouiti and E. A. Assali, "Stability analysis for a class of impulsive bidirectional associative memory (BAM) neural networks with distributed delays and leakage time-varying delays," *Neural Process. Lett.*, vol. 50, no. 1, pp. 851–885, Aug. 2019.
- [16] L. Xiao, B. Liao, S. Li, Z. Zhang, L. Ding, and L. Jin, "Design and analysis of FTZNN applied to the real-time solution of a nonstationary Lyapunov equation and tracking control of a wheeled mobile manipulator," *IEEE Trans. Ind. Informat.*, vol. 14, no. 1, pp. 98–105, Jan. 2018.
- [17] M. Di Marco, M. Forti, P. Nistri, and L. Pancioni, "Discontinuous neural networks for finite-time solution of time-dependent linear equations," *IEEE Trans. Cybern.*, vol. 46, no. 11, pp. 2509–2520, Nov. 2016.
- [18] S. Li, S. Chen, and B. Liu, "Accelerating a recurrent neural network to finite-time convergence for solving time-varying Sylvester equation by using a sign-Bi-power activation function," *Neural Process. Lett.*, vol. 37, no. 2, pp. 189–205, Apr. 2013.
- [19] S. Li, Y. Li, and Z. Wang, "A class of finite-time dual neural networks for solving quadratic programming problems and its k-winners-take-all application," *Neural Netw.*, vol. 39, pp. 27–39, Mar. 2013.
- [20] L. Xiao, Z. Zhang, and S. Li, "Solving time-varying system of nonlinear equations by finite-time recurrent neural networks with application to motion tracking of robot manipulators," *IEEE Trans. Syst., Man, Cybern. Syst.*, vol. 49, no. 11, pp. 2210–2220, Nov. 2019.
- [21] L. Xiao, B. Liao, S. Li, and K. Chen, "Nonlinear recurrent neural networks for finite-time solution of general time-varying linear matrix equations," *Neural Netw.*, vol. 98, pp. 102–113, Feb. 2018.
- [22] S. Li, M. Zhou, X. Luo, and Z. You, "Distributed winner-take-all in dynamic neural networks," *IEEE Trans. Autom. Contr.*, vol. 62, no. 2, pp. 577–589, 2017.
- [23] Q. Xiang, B. Liao, L. Xiao, and L. Jin, "A noise-tolerant Z-type neural network for time-dependent pseudoinverse matrices," *Optik*, vol. 165, pp. 16–28, Jul. 2018.
- [24] D. Chen and Y. Zhang, "Robust zeroing neural-dynamics and its time-varying disturbances suppression model applied to mobile robot manipulators," *IEEE Trans. Neural Netw. Learn. Syst.*, vol. 29, no. 9, pp. 4385–4397, Sep. 2018.
- [25] L. Xiao, J. Dai, R. Lu, S. Li, J. Li, and S. Wang, "Design and comprehensive analysis of a noise-tolerant ZNN model with limited-time convergence for time-dependent nonlinear minimization," *IEEE Trans. Neural Netw. Learn. Syst.*, vol. 31, no. 12, pp. 5339–5348, Dec. 2020.
- [26] Z. Zhang *et al.*, "Robustness analysis of a power-type varying-parameter recurrent neural network for solving time-varying QM and QP problems and applications," *IEEE Trans. Syst., Man, Cybern. Syst.*, vol. 50, no. 12, pp. 5106–5118, Dec. 2020.
- [27] Z. Zhang and L. Zheng, "A complex varying-parameter convergent-differential neural-network for solving online time-varying complex Sylvester equation," *IEEE Trans. Cybern.*, vol. 49, no. 10, pp. 3627–3639, Oct. 2019.
- [28] Z. Zhang, Z. Fu, L. Zheng, and M. Gan, "Convergence and robustness analysis of the exponential-type varying gain recurrent neural network for solving matrix-type linear time-varying equation," *IEEE Access*, vol. 6, pp. 57160–57171, 2018.
- [29] T. Stykel, *Analysis and Numerical Solution of Generalized Lyapunov Equations*. Berlin, Germany: Institut für Mathematik, Technische Universität, 2002.
- [30] C. Mead and M. Ismail, *Analog VLSI Implementation of Neural Systems*, vol. 80. Berlin, Germany: Springer, 2012.
- [31] Z. Hu, L. Xiao, K. Li, K. Li, and J. Li, "Performance analysis of nonlinear activated zeroing neural networks for time-varying matrix pseudoinversion with application," *Appl. Soft Comput.*, vol. 98, Jan. 2021, Art. no. 106735.
- [32] S. Li and Y. Li, "Nonlinearly activated neural network for solving time-varying complex Sylvester equation," *IEEE Trans. Cybern.*, vol. 44, no. 8, pp. 1397–1407, Aug. 2014.
- [33] Z. Tan, W. Li, L. Xiao, and Y. Hu, "New varying-parameter ZNN models with finite-time convergence and noise suppression for time-varying matrix Moore–Penrose inversion," *IEEE Trans. Neural Netw. Learn. Syst.*, vol. 31, no. 8, pp. 2980–2992, Aug. 2020.
- [34] J. J. Craig, *Introduction to Robotics*. 2nd ed. Menlo Park, CA, USA: Addison-Wesley, 1986.



Qiuyue Zuo received the B.S. degree from the School of Mathematical Sciences, Soochow University, Suzhou, China, in 2017. She is currently pursuing the Ph.D. degree with the College of Computer Science and Electronic Engineering, Hunan University, Changsha, China.

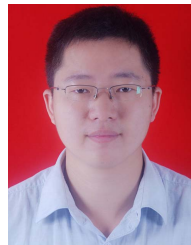
Her main research interests include neural networks and robotics.



Kenli Li (Senior Member, IEEE) received the Ph.D. degree in computer science from the Huazhong University of Science and Technology, Wuhan, China, in 2003.

He was a Visiting Scholar with the University of Illinois at Urbana-Champaign, Champaign, IL, USA, from 2004 to 2005. He is currently a Full Professor of Computer science and electronic engineering with Hunan University, Changsha, China, and also the Deputy Director of the National Supercomputing Center, Changsha. His current research interests

include parallel computing, cloud computing, big data computing, and neural computing.



Lin Xiao received the B.S. degree in electronic information science and technology from Hengyang Normal University, Hengyang, China, in 2009, and the Ph.D. degree in communication and information systems from Sun Yat-sen University, Guangzhou, China, in 2014.

He is currently a Professor with the College of Information Science and Engineering, Hunan Normal University, Changsha, China. He has authored over 100 articles in international conferences and journals. His main research interests include neural networks, robotics, and intelligent information processing.



Keqin Li (Fellow, IEEE) received the B.S. degree in computer science from Tsinghua University, Beijing, China, in 1985, and the Ph.D. degree in computer science from the University of Houston, Houston, TX, USA, in 1990.

He is a SUNY Distinguished Professor of computer science with the State University of New York, New Paltz, NY, USA. He is also a National Distinguished Professor with Hunan University, Changsha, China. He has authored or coauthored more than 780 journal articles, book chapters, and refereed conference articles. He holds nearly 60 patents announced or authorized by the Chinese National Intellectual Property Administration. His current research interests include cloud computing, fog computing and mobile edge computing, energy-efficient computing and communication, embedded systems and cyber-physical systems, heterogeneous computing systems, CPU-GPU hybrid and cooperative computing, machine learning, intelligent, and soft computing.

Dr. Li has received several best paper awards. He has chaired many international conferences. He is currently an Associate Editor of the *ACM Computing Surveys* and the *CCF Transactions on High Performance Computing*. He has served on the Editorial Boards of the *IEEE TRANSACTIONS ON PARALLEL AND DISTRIBUTED SYSTEMS*, the *IEEE TRANSACTIONS ON COMPUTERS*, the *IEEE TRANSACTIONS ON CLOUD COMPUTING*, the *IEEE TRANSACTIONS ON SERVICES COMPUTING*, and the *IEEE TRANSACTIONS ON SUSTAINABLE COMPUTING*.